agriculture

MDPI

Article

Research into Heat Stress Behavior Recognition and Evaluation Index for Yellow-Feathered Broilers, Based on Improved Cascade Region-Based Convolutional Neural Network

Yungang Bai [1], Jie Zhang [1], Yang Chen [2], Heyang Yao [1], Chengrui Xin [1], Sunyuan Wang [2], Jiaqi Yu [2], Cairong Chen [1], Maohua Xiao [1] and Xiuguo Zou [2,*]

[1] College of Engineering, Nanjing Agricultural University, Nanjing 210031, China; 2020112043@stu.njau.edu.cn (Y.B.); 2019812116@stu.njau.edu.cn (J.Z.); 2018812100@njau.edu.cn (H.Y.); 2021112042@stu.njau.edu.cn (C.X.); crchen@njau.edu.cn (C.C.); xiaomaohua@njau.edu.cn (M.X.)

[2] College of Artificial Intelligence, Nanjing Agricultural University, Nanjing 210031, China; 9203020704@stu.njau.edu.cn (Y.C.); 2022819081@stu.njau.edu.cn (S.W.); 32219426@stu.njau.edu.cn (J.Y.)

* Correspondence: zouxiuguo@njau.edu.cn; Tel.: +86-25-58606585

Abstract: The heat stress response of broilers will adversely affect the large-scale and welfare of the breeding of broilers. In order to detect the heat stress state of broilers in time, make reasonable adjustments, and reduce losses, this paper proposed an improved Cascade R-CNN (Region-based Convolutional Neural Networks) model based on visual technology to identify the behavior of yellow-feathered broilers. The improvement of the model solved the problem of the behavior recognition not being accurate enough when broilers were gathered. The influence of different iterations on the model recognition effect was compared, and the optimal model was selected. The final average accuracy reached 88.4%. The behavioral image data with temperature and humidity data were combined, and the heat stress evaluation model was optimized using the PLSR (partial least squares regression) method. The behavior recognition results and optimization equations were verified, and the test accuracy reached 85.8%. This proves the feasibility of the heat stress evaluation optimization equation, which can be used for reasonably regulating the broiler chamber.

Keywords: yellow-feathered broilers; behavior recognition; deep learning; temperature and humidity index; heat stress evaluation equation

check for updates

Citation: Bai, Y.; Zhang, J.; Chen, Y.; Yao, H.; Xin, C.; Wang, S.; Yu, J.; Chen, C.; Xiao, M.; Zou, X. Research into Heat Stress Behavior Recognition and Evaluation Index for Yellow-Feathered Broilers, Based on Improved Cascade Region-Based Convolutional Neural Network. *Agriculture* **2023**, *13*, 1114. https://doi.org/10.3390/agriculture13061114

Academic Editor: Hyeon Tae Kim

Received: 19 April 2023
Revised: 21 May 2023
Accepted: 22 May 2023
Published: 24 May 2023

Copyright: © 2023 by the authors. Licensee MDPI, Basel, Switzerland. This article is an open access article distributed under the terms and conditions of the Creative Commons Attribution (CC BY) license (https://creativecommons.org/licenses/by/4.0/).

1. Introduction

In recent years, with the steady growth in poultry meat production level and consumption, the transformation and upgrading of China's meat and poultry industry have been further accelerated [1]. As one of the main breeds of poultry farming, the breeding scale of yellow-feathered broilers has also expanded [2]. However, the high temperature and humidity in southern China make broilers more prone to heat stress [3], which seriously restricts the large-scale and welfare of the breeding of broilers. Therefore, it is of great significance for broiler breeding to monitor the heat stress state of the broilers and evaluate the corresponding heat stress degree scientifically and effectively.

Heat stress refers to the sum of the non-specific responses of broiler bodies to the high-temperature and high-humidity environment, including physiological and biochemical reactions, behavioral responses, etc. [4]. At present, the environmental parameter method [5] and the behavior analysis method [6] can be used to quickly determine the heat stress of broilers, along with which the THI (temperature and humidity index) [7] is often used within environmental parameters to judge the heat stress, but this is an indirect indicator and cannot accurately assess heat stress. The law of behavior analysis is to judge the state of broilers through behavioral actions. With the development of vision technology and artificial intelligence, the image-based behavior analysis method is being increasingly

applied in poultry farming, which has become an important research field [8]. How to effectively combine broiler behavior and environmental parameters to assess the status of broilers has become an urgent problem to be solved.

Deep learning refers to the combination of multi-layer neural networks to achieve high-level abstraction and data analysis, allowing computers to automatically learn features of a dataset and apply them to tasks such as classification, recognition, and inference [9,10]. The modeling process of heat stress behavior identification and evaluation index prediction models needs to consider image information and temperature, humidity, and other factors, so the establishment of the model is more complicated. Timely monitoring of the health status of broilers is an important premise for broiler welfare feeding, which requires precise classification of various behaviors of broilers. At present, there are two main types of object detection models based on deep learning: a two-stage model based on region recommendation represented by Faster R-CNN (Region-based Convolutional Neural Network), and a one-stage model based on regression represented by YOLO (You Only Look Once). Li et al. [11] used the Faster R-CNN model to detect the stretching behavior of broilers, which can be used for animal welfare assessment. Wang et al. [12] proposed an improved YOLOv3 model to identify five behaviors of broilers, including mating, standing, eating, fighting, and drinking, and the overall average accuracy of the model reached 92.09%. Guo et al. [13] used the lightweight network GhostNet as the backbone of YOLOv4 to analyze the behavior of the pigeons, which greatly reduced the amount of model calculation while ensuring the accuracy of identification. Its recognition speed can reach 0.028 s per frame, and the accuracy rate is 97.06%. Although these models achieve high-precision recognition on conventional objects, a lot of information will be lost when detecting small targets [14].

In highly intensive farming environments, flocks of broilers are crowded together with each other, and event spaces will be limited When extracting images, the broilers are small and numerous, and the adhesion and occlusion are serious, which will cause difficulties in identification. Therefore, most researchers use two-stage object detection models with high accuracy. Li et al. [15] compared the Faster R-CNN and Cascade R-CNN models in detecting greening diseases, and found that Cascade R-CNN outperformed Faster R-CNN by 4.4% and 4.9% in precision and recall, respectively. Dai et al. [16] used HRNet (High-Resolution Net) as the feature extraction network of Cascade R-CNN and combined it with the FPN (Feature Pyramid Network) structure. The average detection accuracy on the test set reached 90.21%, which solves the problems caused by the small size and high density of citrus psyllid. Zhang et al. [17] monitored the behavior of snow leopards based on the improved Cascaded R-CNN object detection model, and the average accuracy increased by 9.0% and 3.9%, respectively, compared with Faster R-CNN and SSD-300. The results show that the improved model based on Cascade R-CNN reaches high detection accuracy for small targets and adhesion groups. Xue et al. [18] proposed an improved Faster R-CNN and introduced the Center Loss supervision signal in the training process of the model to enhance the cohesion of classified features, to improve the recognition accuracy. The results showed that the average accuracy of the model in recognition of pig posture could reach 93.25%. Currently, there are many types of research on the heat stress status of animals, and the evaluation criteria are also different. Aydin et al. [19] and Kristensen et al. [20] successively researched flock activities and the walking posture of single broilers through image technology, to assess the health of broilers. Branco [21] combined behavioral information and temperature and humidity data to study the temporal relationship between heat stress and behavior. Hu et al. [22] studied the influence of temperature on broiler behavior by analyzing the behavior and physiological changes in broilers. They provided a set of criteria for assessing the heat stress level of broilers. Lin et al. [23] used Faster R-CNN to study broiler activities, and combined it with THI value as a predictor of broiler heat stress. Pereira et al. [24] combined machine vision information and temperature and humidity data to propose a clustering index to evaluate the comfort of poultry and to distinguish the difference in broiler aggregation under different temperature conditions.

Ferrari et al. [25] combined sound information from pigs with environmental information and physiological parameters of pigs to demonstrate the feasibility of using continuous sound to assess the heat stress state of pigs. In addition, many researchers have evaluated heat stress in other poultry [26–31].

At present, there is much research on animal behavior analysis combining image information and data information, which can greatly improve the accuracy of poultry behavior analysis compared with the single-image recognition method and the single environmental data monitoring method. However, most of the current image recognition models are applied to larger animals such as pigs, cattle, and sheep. There are still gaps in the identification of broilers and ducks, because poultry are generally small, which cause great challenges to the accuracy of identification. In view of the above problems, this paper proposes an improved Cascade R-CNN model, which introduces an upgraded residual network ResNeXt, which solves the problem of low classification accuracy of the current convolutional neural network model. In addition, the proportion of broiler behavior extracted from the images and the corresponding temperature and humidity information were fitted by the partial least squares regression (PLSR) method to obtain an optimized heat stress evaluation equation, which replaced the original heat stress evaluation equation and can provide a more reliable judgment basis for the assessment of the heat stress environment of the broiler chamber, based on animal behavior information.

2. Materials and Methods

2.1. Introduction to the Experimental Base

The experimental base is located in Jinniuhu Street, Liuhe District, Nanjing, Jiangsu Province, China, and the size of the experimental broiler chamber is 1.9 m × 2.9 m [32]. A video surveillance system and a temperature and humidity monitoring system were installed in the broiler chamber, and the actual picture of the interior is shown in Figure 1. The broilers used in this experiment are only yellow-feathered broilers. Each chamber contained 35 broilers, and each broiler was about 70 days old and weighed 800 g on average. Experiments were conducted in July–August 2019 and July–August 2020.



Figure 1. Top view of the interior of the boiler chamber.

2.2. Video Surveillance System

The video surveillance system consisted of EZVIZ (EZVIZ Network Co., Ltd., Hangzhou, China) CS-C4W-3C2WFR dome network camera, monitoring host, and video recorder to collect real-time video data. The camera had a focal length of 2.8 mm and 2 million pixels, and the captured video pixel was 1920 × 1080. It was mounted on top of the center of the experimental chamber. Figure 2 shows a schematic diagram of video data capture.

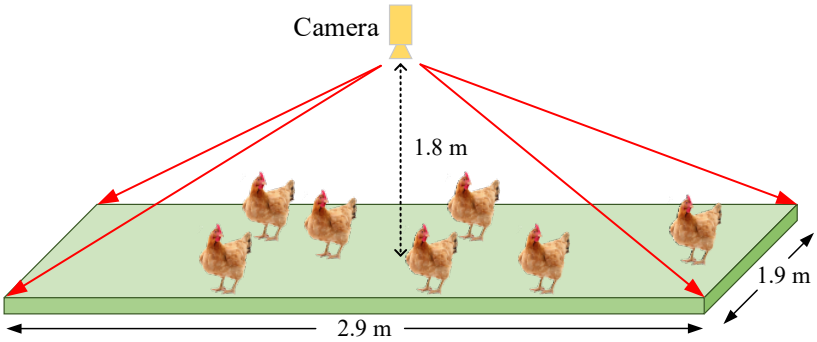


Figure 2. Schematic diagram of video data capture.

2.3. Temperature and Humidity Monitoring System

The experiment used temperature and humidity transmitters to monitor the temperature and humidity in the broiler chamber. The output type of the transmitter was RS485, the measurement accuracy of the temperature and humidity transmitters was ±0.5 °C (25 °C), and ±3% RH, the measurement ranges were −40~+80 °C, and 0%~100% RH, the temperature and humidity resolutions were 0.1 °C and 0.1% RH, the data update time was 2 s, and the sampling frequency was 1 time/min. The instrument was installed 30 cm from the bottom of the broiler chamber to monitor the living layer environmental data of the broilers. The monitoring instruments are shown in Figure 3.



Figure 3. Temperature and humidity transmitter and air quality transmitter in the broiler chamber.

2.4. Data Collection and Image Dataset Production

During the experiment from July to August 2019, the above video surveillance system and temperature and humidity monitoring system were used for data collection. Considering that welfare breeding needs to meet the most basic natural needs of broilers, the LED lights in the broiler chamber were turned off from 11:00 pm to 5:00 am of the next day, which was the rest time for the broilers. Therefore, the data were collected during the daylight period of 5:00 am~11:00 pm.

2.4.1. Behavioral Definition of Broilers

Broilers change their behavior and diet in high-temperature environments to regulate body temperature. Under the influence of heat stress, broilers will exhibit the behavior of raising their wings and lying prone on the ground to enhance the heat dissipation effect and ensure the stability of their body temperature, which can be regarded as a direct behavior from heat stress. In addition, broilers' water intake increases and pecking decreases, which can be seen as an indirect behavior from the heat stress on broilers [33]. According to the actual situation and the effect of heat stress on broilers, the behavior of yellow-feathered broilers was divided into eating, drinking, heat stress (wings raised or prone on the ground), and others. The definition of the behavior is shown in Table 1.

Table 1. Different behavioral definitions of yellow-feathered broilers.

Behavior Classification	Classification Definition
Eating	The head of the yellow-feathered broiler protrudes into the feeding trough and makes contact with the feeding trough.
Drinking	The head of the yellow-feathered broiler protrudes into the sink and cup, and makes contact with the sink or cup.
Heat Stress	The wings of the yellow-feathered broiler are apparently raised, or the broiler is prone on the ground.
Others	This includes actions such as standing, walking, and preening.

Among these, 'heat stress' indicates a direct response to heat stress, 'eating' and 'drinking' could indicate indirect reactions to heat stress, and 'others' indicates that the broilers do not respond to heat stress. A schematic of the behavior is shown in Figure 4.



(**a**) (**b**) (**c**) (**d**)

Figure 4. Different behavior images of yellow-feathered broilers: (**a**) Eating; (**b**) Drinking; (**c**) Heat Stress; (**d**) Others.

2.4.2. Acquisition and Annotation of Experimental Data

This experiment on the behavior recognition of yellow-feathered broilers was carried out with a constant number of broilers in one chamber. The interference of human factors in the collected video information was eliminated by screening (including adding food, adding water, overhauling the internal equipment of the broiler chamber, etc.). Videos were exported corresponding to different periods every day. Considering the smooth progress of the follow-up research of this experiment, in the process of converting video data into image data, the image information corresponded to the temperature and humidity information, according to the time relationship. Taking the naming of the first image, for example, the name was indicated as the first image taken from 5:30 pm on 6 August 2019, the following 33.1 is the temperature at the corresponding time, and 60.2 is the corresponding humidity data. Frame images were acquired in chronological order and named according to the criteria described above. The image was annotated using Labelme and converted into PASCAL VOC formats for subsequent research. After image preprocessing (resizing, random flipping, translation transformation.), a total of 6241 images were obtained. The dataset was divided into a training set, a validation set, and a test set, according to the ratio of 8:1:1

2.5. Recognition Model of Heat Stress Behavior in Yellow-Feathered Broilers

2.5.1. Model Network Structure

Object detection technology has been developed for nearly 20 years, with AlexNet as the dividing line; traditional machine algorithms were mainstream before 2012. Since 2013, deep learning algorithms have gradually become popular [34]. Currently, the object detection algorithm based on deep learning is divided into two types, one-stage and two-stage, and the one-stage model has fast detection speed, so the recognition accuracy rate is low. While the two-stage model runs slowly, it has advantages in recognition accuracy. Since the accuracy of various types of behavior recognition of broilers will directly affect

the calculation results of the THI value, this paper adopted a two-stage model with higher accuracy. The R-CNN series models are typical two-stage object detection models. This paper selects the current mainstream Cascade R-CNN as the basic network.

The feature extraction backbone network of Cascade R-CNN is ResNet, which can solve the accuracy degradation problem and gradient vanishing problem when training with a multilayer network, through residual learning. However, the ResNet model also has some drawbacks. For example, reducing the downsampling factors will reduce the effective receptive field, which is not conducive to the model detecting small targets, and it will consume a lot of time and memory in maintaining the spatial resolution of deep neural networks.

To solve the above problems, this article makes the following improvements to the Cascade R-CNN model. On the one hand, ResNext is used to replace the original feature extraction network, which can reduce the number of hyperparameters and ensure the accuracy of the model. On the other hand, this paper embeds FPN (Feature Pyramid Network) into the RPN (Region Proposal Network), generating features of different scales and fusing them as inputs for the RPN network. Different sizes of anchors are defined at each scale layer. By effectively fusing the high-resolution shallow layers with rich semantic information in the deep layers, the computational efficiency is improved, overfitting is reduced, and the detection ability for small targets is further enhanced. The above improvements can effectively solve the problem of low recognition accuracy caused by the small proportion and close aggregation of broiler targets in the image. The improved network structure is shown in Figure 5.

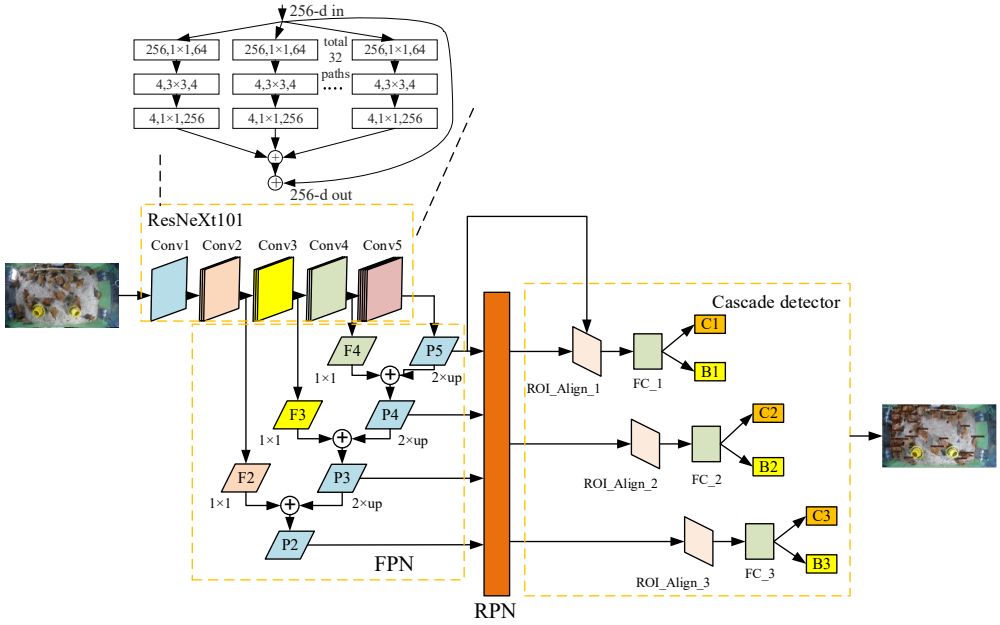


Figure 5. Network structure diagram of improved Cascade R-CNN.

2.5.2. Model Training Parameters

The stochastic gradient descent method was used with a batch value of 50. This paper adopted the learning rate update strategy. The initial value of the learning rate was set to 0.02, the momentum factor was set to 0.9, and the weight decay rate was 0.0001. This training had a total of 12 epochs and more than 89,000 iterations. The hardware platform for this training was configured with a Tesla V100 graphics card with 32 G of memory and an Intel Xeon Gold 6130 CPU with 128 G of memory. The Python version is 3.7, and the PyTorch framework version is 1.7.1.

2.5.3. Model Evaluation Metrics

This experiment used two evaluation indicators: mAP (mean average precision) and recall. mAP measures the recognition performance of the model for all classes. Recall is a measure of the model's ability to cover broiler behavior detection, and is the proportion of broilers identified from all broilers.

The model precision, recall, average precision, and mAP are calculated as follows: Equations (1)–(4) [35]:

$$\mathrm{P} = \frac{\mathrm{TP}}{\mathrm{TP} + \mathrm{FP}} \tag{1}$$

$$\mathrm{R} = \frac{\mathrm{TP}}{\mathrm{TP} + \mathrm{FN}} \tag{2}$$

$$\mathrm{AP} = \sum_{k=1}^{\mathrm{N}} \mathrm{P}(k)\Delta\mathrm{R}(k) \tag{3}$$

$$\mathrm{mAP} = \frac{1}{\mathrm{C}} \sum_{k=1}^{\mathrm{N}} \mathrm{P}(k)\Delta\mathrm{R}(k) \tag{4}$$

where TP is the true positive sample, FP is the false positive sample, FN is the false negative sample, C represents the number of target classes detected, k is the class serial number, N is the total number of samples, $\mathrm{P}(k)$ is the accuracy corresponding to the first k samples, and $\Delta\mathrm{R}(k)$ is the change value of the recall of the first k samples corresponding to the first $k-1$ samples.

Formal approaches are becoming increasingly important for verifying AI-based object detection techniques, which can be used to exhaustively check the performance of the model. These approaches rely on mathematical models and logic to check system correctness, and can help ensure that object detection models are reliable and accurate. Model checking can be used to systematically verify whether a deep learning model satisfies specific requirements. Theorem proving can be used to verify the correctness of the underlying algorithms. In this paper, precision, recall, and average precision were selected to check the model [36,37].

2.6. Heat Stress Assessment Model

2.6.1. Heat Stress Evaluation Index

In the case of high temperature and humidity in summer, the broiler's body temperature is too high, and it is impossible to return to the thermoneutral state, which can easily cause heat stress. The heat stress index THI was obtained by combining temperature and relative humidity, and was used to indicate the degree of heat stress in broilers. The heat stress index of broilers first used in this research is shown in Equation (5) [38]:

$$\mathrm{THI} = \mathrm{T}{*}1.8 + 32 + \mathrm{RH} \tag{5}$$

where T represents the ambient temperature, and RH represents the ambient humidity. When the heat stress index is lower than 150, broilers will not suffer from heat stress; 155 is a threshold, beyond which broilers will produce a stress response. This paper used deep-learning-based visual techniques to identify broiler behavior and combined the traditional temperature humidity index method to evaluate heat stress. It was able to more accurately assess the heat stress status of broilers by optimizing the evaluation index of heat stress.

2.6.2. Numerical Dataset Production

Python code was used to count the percentage of broilers with different behaviors in the JSON file, and the temperature and humidity data were extracted. They were saved in an Excel table after combining image data and temperature and humidity data.

Data screening: the image of the first second of each minute in the video was preserved, and the rest was culled as redundant data, to ensure the rationality of this dataset. Each sub-dataset included the number of individual behaviors of broilers in the image and corresponding temperature and humidity data. A total of 573 new datasets were obtained.

Data normalization: the environmental parameter and behavior analysis methods for heat stress evaluation have different evaluation indicators. In order to eliminate the dimensional influence between indicators, data normalization is required, so that each index is in the same order of magnitude, suitable for comprehensive comparative evaluation. The transfer function is shown in Equation (6).

$$x_{norm} = \frac{x - x_{min}}{x_{max} - x_{min}} \tag{6}$$

where x_{max} and x_{min} represent the maximum and minimum values of the data, respectively.

3. Results and Analysis

3.1. The Effect of Different Iterations on the Model's Performance

During the model training process, the curve of the loss function intuitively reflects the dynamic training process and the network's convergence. The loss curve of the training model is shown in Figure 6. The curve shows the changing trend of the loss function during the whole training process. In the first 2000 iterations, the loss value decreased rapidly. After 60,000 iterations, the curve still showed a significant change, and then the loss value tended to stabilize, indicating that the network convergence effect was ideal.

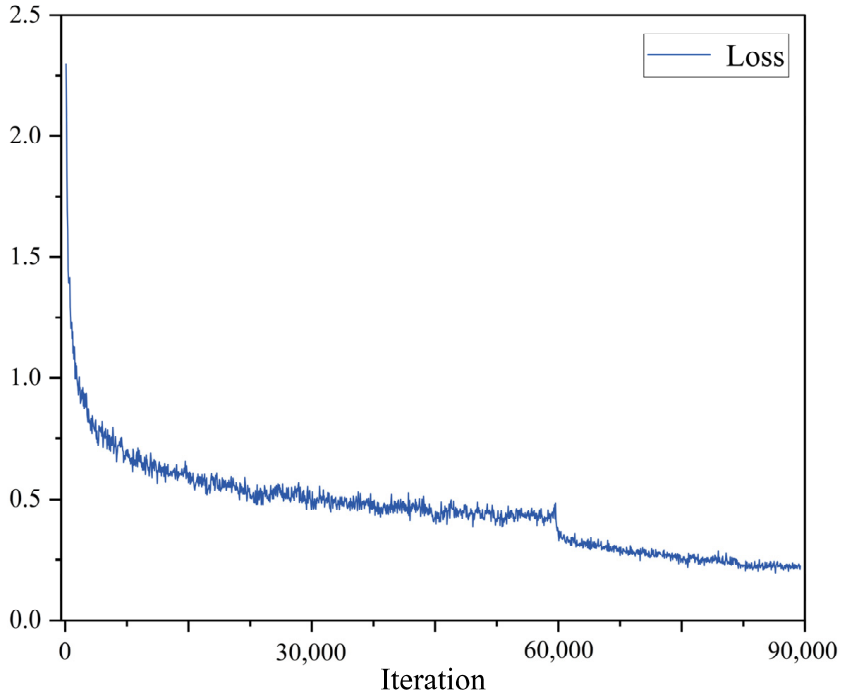


Figure 6. Training loss curve of the improved algorithm.

The mAP line chart trained by the improved Cascade R-CNN model, Cascade R-CNN model, and Faster R-CNN model is shown in Figure 7. It can be seen that the mAP of the improved model is higher than that of the Cascade R-CNN model and the Faster R-CNN model, after multiple training. The mAP of the improved Cascade R-CNN model can reach 0.882, which has better recognition performance than the other two. It can be seen that the improved model improves recognition accuracy.

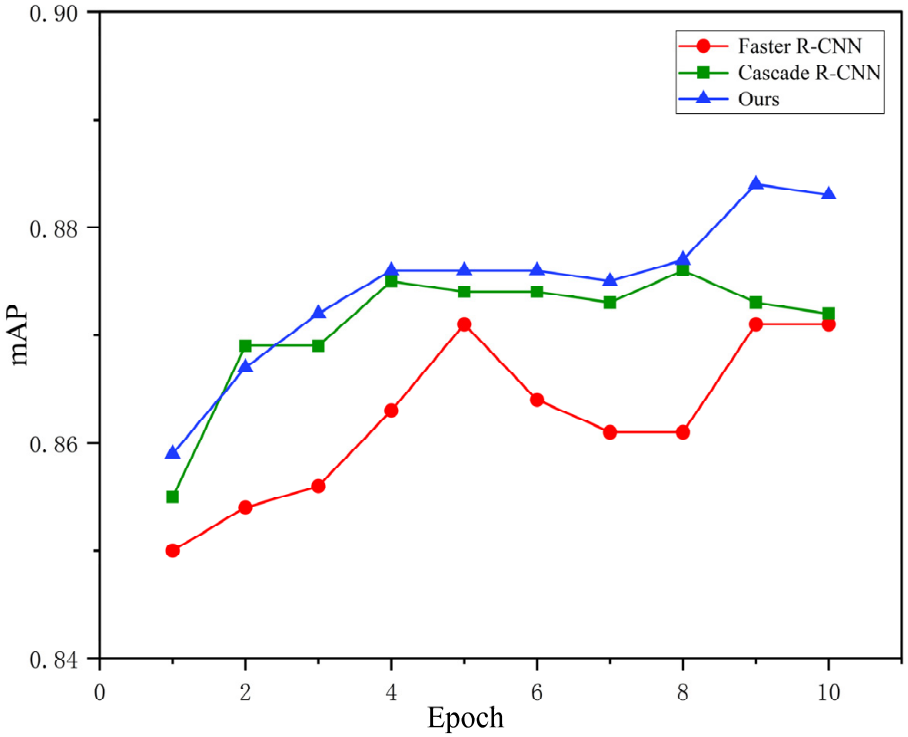


Figure 7. The training mAP line graph of different experimental models.

In general, the performance of the model will improve as the number of iterations increases during the training process. However, too much training may lead to overfitting, so it is necessary to evaluate the trained model. During training, one model is output every 7488 iterations (i.e., one epoch). In this research, the last five models of the iteration were selected for analysis, and Model 1~Model 5 are shown in Table 2.

Table 2. Comparison of model performance at different iterations.

Model	Iterations	mAP	Recall
1	59,904	0.877	0.970
2	67,392	0.884	0.956
3	74,880	0.883	0.955
4	82,368	0.882	0.945
5	89,856	0.882	0.946

As can be seen from Table 2, Model 2 performs best when the number of iterations is 67,392. At this time, the learning rate is 0.002, the loss value is 0.2842, and the mAP is higher than the other four groups of models, while the recall rate is slightly lower than the 0.970 of Model 1. As the training continues, the mAP and recall decrease, and the model overfits, so Model 2 is used as the optimal model.

The prediction results of the Cascade R-CNN model and the improved model for the same image are shown in Figures 8 and 9, respectively. It can be seen that the Cascade R-CNN model can identify the most gathered broilers before the improvement, but there are still errors in the judgment of the behavior of gathering broilers. Meanwhile, the improved model has a good recognition performance on broilers with a high degree of aggregation, and can also correctly identify broilers with unclear features.



Figure 8. Recognition result of the Cascade R-CNN.



Figure 9. Recognition result of the improved model.

3.2. Environmental Conditions Change

The temperature and humidity data of 20 July 2019, 1 August 2019, and 9 August 2019 were selected to calculate the heat stress index according to Equation (5). As shown in Figure 10, the THI value is basically above the critical point of 155, which indicates that the yellow-feathered broilers were in a heat stress environment in summer. However, the response of the broilers does not match the experimental results, which shows that the original equation could not accurately reflect the heat stress environment. Therefore, the calculation equation of THI for heat stress assessment needs to be optimized, in combination with behavioral responses.

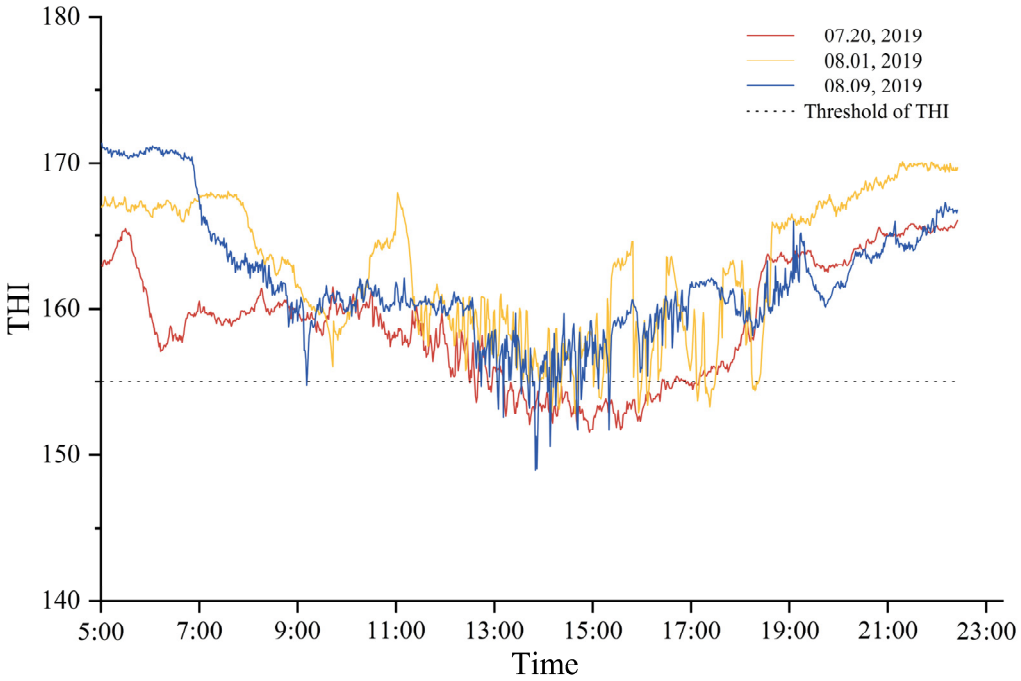


Figure 10. Assessment curves of heat stress index at different dates.

3.3. Heat Stress Assessment Model Optimization

3.3.1. Establishment of Evaluation Model

The Ridge regression method and the PLSR method were used to establish the evaluation model in this research. The Ridge regression loses part of the information and reduces the accuracy, which makes the regression coefficient more realistic and reliable, and it can effectively deal with the collinearity problem between variables. The PLSR method was used to establish the evaluation model in this research, which found the best matching function for the data by minimizing the sum of squared errors. It synthesizes and screens the information in the regression modeling process, extracts the components with the best explanatory ability for the system, and then performs regression modeling to obtain the truth values most conveniently.

When modeling with the multiple linear regression analysis method, it is especially important to determine the optimal number of potential variables to participate in regression. If fewer variables are selected, the adjustment model will not fit adequately. If too many variables are selected, it will cause the adjustment model to overfit. The experiment used the LOOCV (leave-one-out cross-validation). It determined that the best number of potential variables of the model is two, based on the minimum value of the sum of squares of the predicted residuals. The sample set was divided into a training set and a test set, using the SPXY method (sample set partitioning based on joint x–y distance), with a ratio of 3:1. Among them, the number of samples in the correction set was 430, and the number of samples in the test set was 143.

The calculation was mainly divided into the following parts: finding the correlation coefficient matrix, extracting the components of the independent variable group and the dependent variable group, finding the regression equation of the index variable and the component variable, and finding the regression equation between the independent variable and the dependent variable.

Equation (7) obtained by the PLSR regression method:

$$THI1 = 29.565 + 1.912T + 0.85RH + 10.562HS - 2.542E + 5.586D - 0.458O \quad (7)$$

Equation (8) obtained from the Ridge regression method:

$$\mathrm{THI2} = 96.077 + 0.871\mathrm{T} + 0.512\mathrm{RH} - 17.925\mathrm{E} + 4.353\mathrm{HS} - 3.712\mathrm{O} + 27.087\mathrm{D} \quad (8)$$

where T represents the ambient temperature, RH represents the ambient humidity, E represents the proportion of broilers that are eating, HS represents the proportion of broilers suffering from heat stress, O represents the proportion of broilers in the 'others' state, and D represents the proportion of broilers that are drinking.

3.3.2. Test of Evaluation Model Performance

The above equations are compared according to the coefficient of determination R^2 and the RMSE (root-mean-square error). The expressions are shown in Equations (9) and (10):

$$R^2 = 1 - \frac{\sum_{i=1}^{m}(y_i - \hat{y})^2}{\sum_{i=1}^{m}(y_i - \overline{y_l})^2} \quad (9)$$

$$\mathrm{RMSE} = \sqrt{\frac{1}{m}\sum_{i=1}^{m}(y_i - \hat{y})^2} \quad (10)$$

where y_i is the actual value of the heat stress index, $\hat{y}$ is the predicted value of the heat stress index, and $\overline{y_l}$ is the average of the actual value of the heat stress index. The quality of the model is judged by R^2, which generally ranges from (0, 1). When the R^2 value is 1, the fitting performance is best, and RMSE indicates how well the measured value fits the actual value curve. A low RMSE value means that the model has high measurement accuracy.

The model test results are shown in Table 3. The R^2 value obtained according to Equation (7) is 0.7832, while the R^2 value obtained according to Equation (8) is 0.6412, indicating that the fitting result is not satisfactory and does not meet the actual needs. In addition, the RMSE value calculated according to Equation (7) is 6.4051, while the RMSE value calculated according to Equation (8) is 4.9459. The obtained evaluation equation will calculate the THI value, according to the actual situation. Therefore, we pay more attention to the interpretability and fit of the model and less attention to the prediction accuracy of the model, so we think that R^2 is a more important evaluation index. To sum up, the equation obtained according to the PLSR method describes the heat stress state of broilers better.

Table 3. Comparison of validation results of evaluation models obtained by different methods.

Equation	R^2	RMSE
THI1	0.7832	6.4051
THI2	0.6412	4.9459

The fitted curve plots between the predicted and actual values obtained by the partial least squares regression method and the Ridge regression analysis method are shown in Figures 11 and 12.

It can be seen from the graph that the equation obtained by the PLSR method fits better; the actual values and predicted values are closer, so Equation (7) was selected as the optimization equation for temperature and humidity data, combined with behavioral variables.

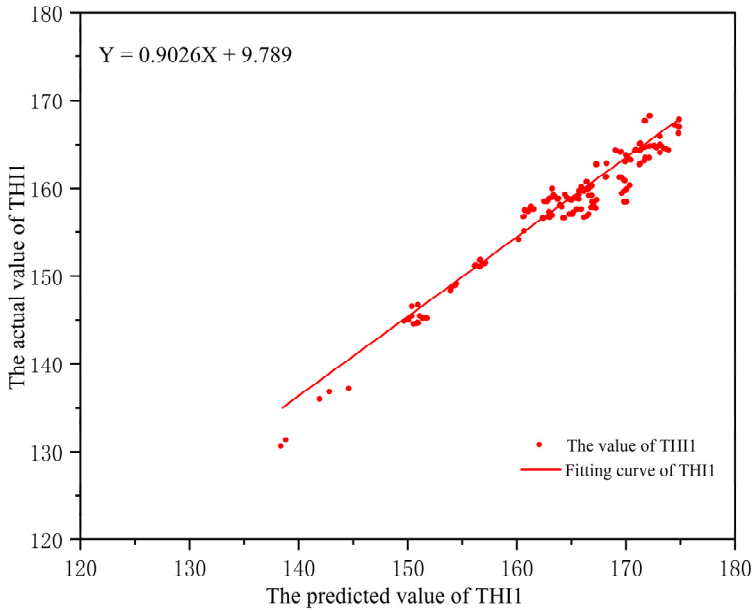


Figure 11. Chart of the fitting curve between the predicted value and actual value of THI1.

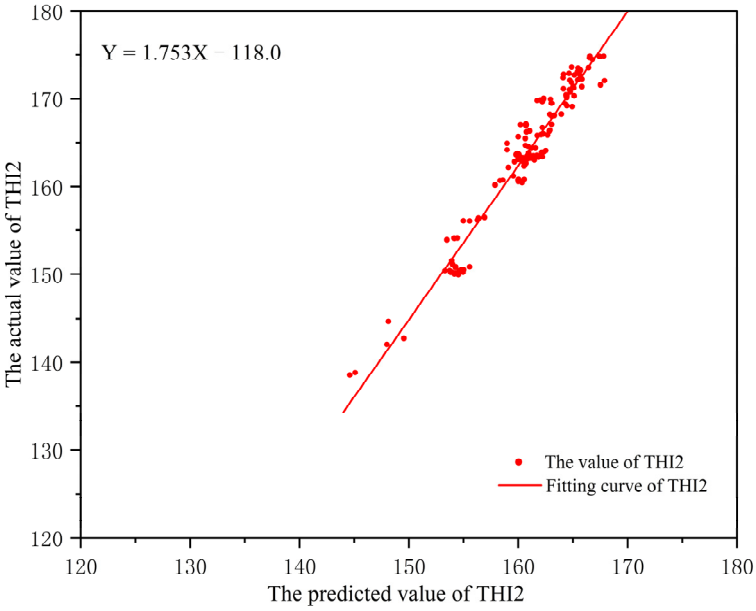


Figure 12. Chart of the fitting curve between the predicted value and actual value of THI2.

3.4. Experimental Analysis

3.4.1. Algorithmic Model Experimentation

In order to test the performance of the model in actual application, images of 10, 20, and 30 yellow-feathered broilers were selected for behavioral recognition model testing. The test results are shown in Figures 13–15.

From the figures above, it can be found that the improved model based on Cascade R-CNN can accurately identify the different behaviors of broilers when broilers gather, and the features of the broilers are not obvious. Its recognition effect is better.

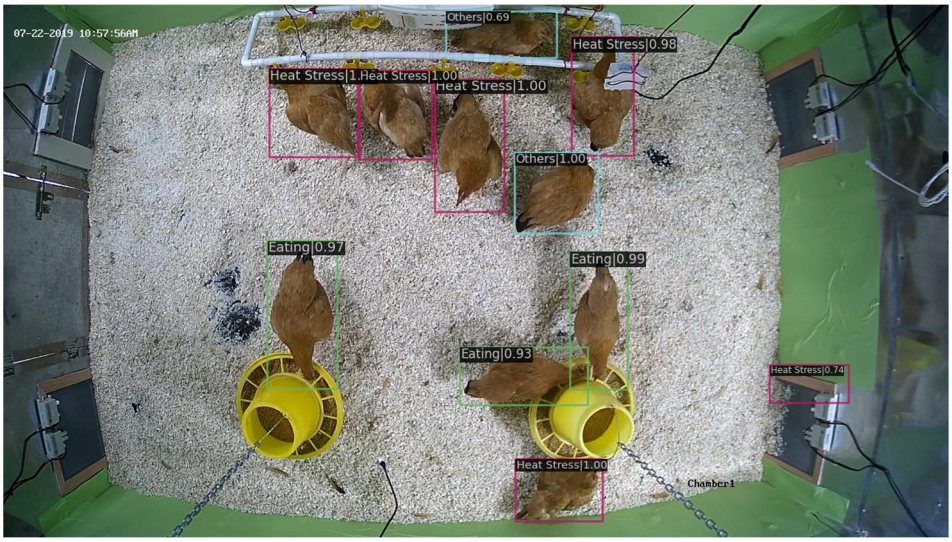


Figure 13. Recognition result of the improved model for 10 broilers.

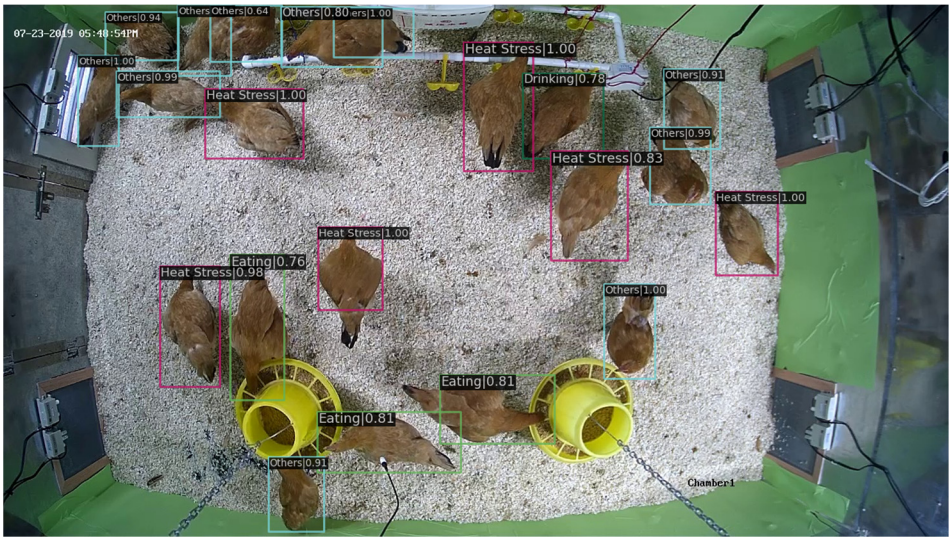


Figure 14. Recognition result of the improved model for 20 broilers.

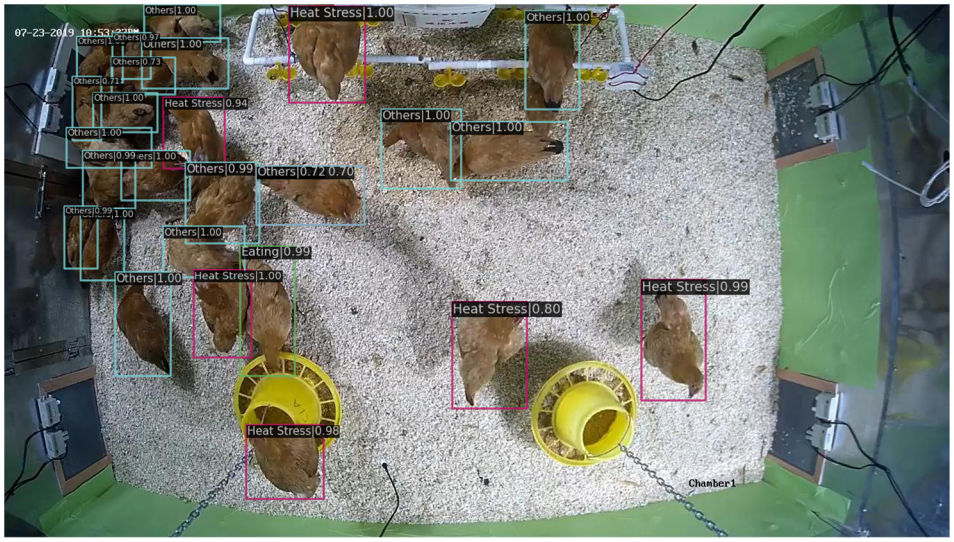


Figure 15. Recognition result of the improved model for 30 broilers.

3.4.2. Evaluation of Model Experiments

The behavior recognition results were applied to Equation (7) for verification analysis. Based on the experimental results in Table 2, five images were randomly selected to test the performance of Model 2. The test results and corresponding temperature and humidity information are shown in Table 4.

Table 4. Behavior recognition results and corresponding temperature and humidity information.

Image Set	Eating (E)/%	Drinking (D)/%	Heat Stress (HS)/%	Others (O)/%	Temperature (T)/°C	Relative Humidity (RH)/%	THIa	THIb
1	3.2	0	41.9	54.9	33.7	58.1	147.48	150.76
2	8.6	14.3	51.4	25.7	33.9	68.3	158.33	161.32
3	5.7	14.3	42.9	37.1	33.4	63.5	152.41	155.62
4	5.7	11.4	48.6	34.3	33.8	67.5	157.03	160.34
5	0	11.4	57.1	31.5	32.8	80.4	167.15	171.44

According to the temperature and humidity index a_i obtained by the optimization Equation (7) and the temperature and humidity index b_i obtained by the original heat stress evaluation Equation (5), the data are verified, and the accuracy of the heat stress evaluation (HE) is shown in Equation (11).

$$\mathrm{HE} = \mathrm{mAP}_{\mathrm{best}} \times \frac{\sum_{i=1}^{\mathrm{n}} \frac{a_i}{b_i}}{\mathrm{n}} \tag{11}$$

where $\mathrm{mAP}_{\mathrm{best}}$ is the average accuracy of Model 2 used, and the value is 88.4%. n is the number of randomly selected images, and a_i/b_i is the ratio of the data obtained by the optimization equation to the data obtained by the original evaluation equation.

In this experiment, a total of 20 sets of images were randomly selected to calculate the heat stress evaluation (HE) of Equation (7); the highest accuracy was 86.5%, and the corresponding information is shown in Table 4. After calculation, the heat stress index calculated by the original equation and the optimized equation is basically the same, and the average HE reached 85.8%. It can be seen that the optimization equation can be used to evaluate heat stress environments more accurately and realize the monitoring of the heat stress status of broilers during the summer breeding process.

4. Conclusions

(1) This paper proposed a novel method for detecting the heat stress behavior of broilers by combining images with temperature and humidity data. On the one hand, due to the diversity of animal behavior, relying solely on image recognition technology to detect and define complex behaviors such as heat stress may lead to problems such as false positives and false negatives. On the other hand, there are individual differences among animals, and under the same external environmental conditions, the response of broilers can vary greatly. If only temperature and humidity data are used for overall regulation, some broilers with special reactions may be ignored. Therefore, the broiler heat stress detection method proposed in this paper, which combines images and data, can effectively overcome the shortcomings of these two methods.

(2) The specific improvements in this paper are summarized below. First, an improved Cascade R-CNN model was proposed to identify broiler behavior by introducing the ResNeXt network, which solves the problem of low classification accuracy of the current CNN model. The computational efficiency of the improved model is greatly improved, and the final mAP reached 88.4%, which is significantly improved compared with the Cascade R-CNN model and the Faster R-CNN model. In addition, the proportion of broiler behavior and the corresponding temperature and humidity values were extracted from the data collected from the broiler chamber. The evaluation model was optimized by the PLSR method combined with behavioral variables and temperature and humidity, and the test accuracy reached 85.8%. The results show that

the optimization equation can accurately evaluate the heat stress environment, based on the behavior of broilers. This method replaces the original heat stress evaluation equation, which can accurately monitor the heat stress of broilers in the chamber and provide a more reliable basis for the subsequent judgment of broiler heat stress.

(3) This method has achieved good performance in the small-scale breeding experiment in the first three months of the growth cycle of yellow-feathered broilers, and can be applied to large-scale yellow-feathered-broiler breeding in the future; non-invasive image acquisition devices and temperature and humidity sensors can monitor the health status of the broiler while minimizing the impact on the normal life of poultry, and promote the automation and intelligent development of the poultry breeding industry. In the future, the accuracy of the behavior recognition model needs to be further improved, especially when applied to large-scale yellow-feathered-broiler breeding, as the occlusion among broilers will be serious, which will affect the results of image recognition. In addition, more environmental parameters related to broiler heat stress will be considered in calculating the evaluation model (such as carbon dioxide concentration, atmospheric pressure, etc.), and will improve the reliability of model identification in different environments.

Author Contributions: Conceptualization, X.Z.; data curation, Y.B., J.Z., H.Y., C.X. and X.Z.; formal analysis, Y.B., J.Z., Y.C., C.X., S.W., J.Y. and X.Z.; funding acquisition, X.Z.; methodology, Y.B., J.Z., Y.C., H.Y. and X.Z.; project administration, M.X. and X.Z.; supervision, X.Z.; visualization, Y.B. and J.Z.; writing—original draft, Y.B., J.Z., Y.C., H.Y., C.X., S.W. and X.Z.; writing—review and editing, C.C., M.X. and X.Z. All authors have read and agreed to the published version of the manuscript.

Funding: This research was funded by the Jiangsu Agriculture Science and Technology Innovation Fund of China (CX(21)3058), the Program for International S&T Cooperation Projects of Jiangsu, China (BZ2021022).

Institutional Review Board Statement: Not applicable.

Data Availability Statement: Not applicable.

Acknowledgments: We are thankful to Yuanyuan Song, Wenchao Liu, Chenyang Wang and Zhilong Chen, who have contributed to our field data collection and primary data analysis.

Conflicts of Interest: The authors declare no conflict of interest.

References

1. Lao, F.; Teng, G.; Li, J.; Yu, L.; Li, Z. Behavior recognition method for individual laying hen based on computer vision. *Trans. Chin. Soc. Agric. Eng.* **2012**, *28*, 157–163. [CrossRef]
2. Shi, Z.; Xi, L.; Ji, Z.; Cheng, P. LED illuminant improving broilers house environment and growth performance. *Trans. Chin. Soc. Agric. Eng.* **2017**, *33*, 222–227. [CrossRef]
3. Yan, G.; Li, H.; Shi, Z.; Wang, C. Research status and existing problems in establishing cow heat stress indices. *Trans. Chin. Soc. Agric. Eng.* **2019**, *35*, 226–233.
4. Iyasere, O.; Oyetunji, D.E.; Wheto, M.; Durosaro, S.; Adigun, T.; Muraina, O.; Daramola, J. Effect of acute heat stress on cognitive performance of chickens in a feed-related discriminant task. *J. Therm. Biol.* **2021**, *98*, 102914. [CrossRef]
5. Min, Q.; Xiao, J.; Shao, Z. Influence of temperature and humidity on layer's productivity and hot stress index. *J. Nanjing Inst. Meteorol.* **1994**, *17*, 367–371.
6. Saeed, M.; Abbas, G.; Alagawany, M.; Ali, A.; Sun, C. Heat stress management in poultry farms: A comprehensive overview. *J. Therm. Biol.* **2019**, *84*, 414–425. [CrossRef]
7. Thom, E. The discomfort index. *Weatherwise* **1959**, *12*, 57–61. [CrossRef]
8. Cangar, Ö.; Leroy, T.; Guarino, M.; Vranken, E.; Fallon, R.; Lenehan, R.; Mee, J.; Berckmans, D. Automatic real-time monitoring of locomotion and posture behaviour of pregnant cows prior to calving using online image analysis. *Comput. Electron. Agric.* **2008**, *64*, 53–60. [CrossRef]
9. Geng, Z.; Zhao, Z.; Shi, Y.; Wu, X.; Formel, S.; Sen, M. Deep learning for velocity model building with common-image gather volumes. *Geophys. J. Int.* **2022**, *228*, 1054–1070. [CrossRef]
10. Shen, F.; Zhao, X.; Kou, G.; Alsaadi, F. A new deep learning ensemble credit risk evaluation model with an improved synthetic minority oversampling technique. *J. Therm. Biol.* **2021**, *98*, 106852. [CrossRef]

11. Li, G.; Zhao, Y.; Porter, Z.; Purswell, J. Automated measurement of broiler stretching behaviors under four stocking densities via faster region-based convolutional neural network. *Animal* **2021**, *15*, 100059. [CrossRef] [PubMed]
12. Wang, J.; Wang, N.; Li, L.; Ren, Z. Real-time behavior detection and judgment of egg breeders based on YOLO v3. *Neural Comput. Appl.* **2020**, *32*, 5471–5481. [CrossRef]
13. Guo, J.; He, G.; Deng, H.; Fan, W.; Xu, L.; Cao, L.; Feng, D.; Li, J.; Wu, H.; Lv, J.; et al. Pigeon cleaning behavior detection algorithm based on lightweight network. *Comput. Electron. Agric.* **2022**, *199*, 107032. [CrossRef]
14. Chen, C.; Liu, M.; Tuzel, O.; Xiao, J. R-CNN for small object detection. In *Computer Vision–ACCV 2016: Proceedings of the 13th Asian Conference on Computer Vision, Taipei, Taiwan, 20–24 November 2016*; Springer International Publishing: Cham, Switzerland, 2017; pp. 214–230. [CrossRef]
15. Li, M.; Lee, S. A study on small pest detection based on a Cascade R-CNN-Swin model. *CMC-Comput. Mater. Contin.* **2022**, *72*, 6155–6165.
16. Dai, F.; Wang, F.; Yang, D. Detection method of citrus psyllids with field high-definition camera based on improved cascade region-based convolution neural networks. *Front. Plant Sci.* **2022**, *12*, 3136. [CrossRef]
17. Zhang, Y.; Gao, Y.; Chang, F.; Xie, J.; Zhang, J. Automatic detection of snow leopard (*Panthera uncia*) at species level based on improved Cascade R-CNN. *Chin. J. Wildl. Trans. CSAE* **2022**, *43*, 307–313. [CrossRef]
18. Xue, Y.; Zhu, X.; Zheng, C.; Mao, L.; Yang, A.; Tu, S.; Huang, N.; Yang, X.; Chen, P.; Zhang, N. Lactating sow postures recognition from depth image of videos based on improved Faster R-CNN. *Chin. J. Wildl. Trans. CSAE* **2018**, *34*, 189–196. [CrossRef]
19. Aydin, A.; Cangar, O.; Ozcan, S.; Bahr, C.; Berckmans, D. Application of a fully automatic analysis tool to assess the activity of broiler chickens with different gait scores. *Comput. Electron. Agric.* **2010**, *73*, 194–199. [CrossRef]
20. Kristensen, H.; Cornou, C. Automatic detection of deviations in activity levels in groups of broiler chickens—A pilot study. *Biosyst. Eng.* **2011**, *109*, 369–376. [CrossRef]
21. Branco, T.; Moura, D.; Nääs, I.; Oliveira, S. Detection of broiler heat stress by using the generalised sequential pattern algorithm. *Biosyst. Eng.* **2020**, *199*, 121–126. [CrossRef]
22. Hu, C.; Zhang, M.; Feng, J.; Su, H.; Zhang, S. Effects of thermal stimulation on resting behavior, physiology and performance of broilers. *Chin. J. Anim. Nutr.* **2015**, *27*, 2070–2076. [CrossRef]
23. Lin, C.; Hsieh, K.; Tsai, Y.; Kuo, Y. Automatic monitoring of chicken movement and drinking time using convolutional neural networks. *Trans. ASABE* **2020**, *63*, 2029–2038. [CrossRef]
24. Pereira, D.; Lopes, A.; Filho, G.; Salgado, D.; Neto, M. Cluster index for estimating thermal poultry stress (*Gallus gallus domesticus*). *Comput. Electron. Agric.* **2020**, *177*, 105704. [CrossRef]
25. Ferrari, S.; Costa, A.; Guarino, M. Heat stress assessment by swine related vocalizations. *Livest. Sci.* **2013**, *151*, 29–34. [CrossRef]
26. Ribeiro, B.; Junior, T.; Oliveira, D.; Lima, R.; Zangeronimo, M. Thermoneutral zone for laying hens based on environmental conditions, enthalpy and thermal comfort indexes. *J. Therm. Biol.* **2020**, *93*, 102678. [CrossRef] [PubMed]
27. Siriani, A.; Kodaira, V.; Mehdizadeh, S.; Naas, I.; Moura, D.; Pereira, D. Detection and tracking of chickens in low-light images using YOLO network and Kalman filter. *Neural Comput. Appl.* **2022**, *34*, 21987–21997. [CrossRef]
28. Mader, T.; Davis, M.; Brown, B. Environmental factors influencing heat stress in feedlot cattle. *J. Anim. Sci.* **2006**, *84*, 712–719. [CrossRef]
29. Jeelani, R.; Konwar, D.; Khan, A.; Dhirendra, K.; Dibyendu, C.; Biswajit, B. Reassessment of temperature-humidity index for measuring heat stress in crossbred dairy cattle of a sub-tropical region. *J. Therm. Biol.* **2019**, *82*, 99–106. [CrossRef]
30. Tsai; Yu, C.; Jih, T.; Shih, T.; Dan, J.; Ta, T. Assessment of dairy cow heat stress by monitoring drinking behaviour using an embedded imaging system. *Biosyst. Eng.* **2020**, *199*, 97–108. [CrossRef]
31. Okinda, C.; Lu, M.; Liu, L.; Nyalala, I.; Muneri, C.; Wang, J.; Zhang, H.; Shen, M. A machine vision system for early detection and prediction of sick birds: A broiler chicken model. *Biosyst. Eng.* **2019**, *188*, 229–242. [CrossRef]
32. Yao, H.; Sun, Q.; Zou, X.; Wang, S.; Zhang, S. Research of yellow-feather broiler breeding model based on small broiler. *INMATEH-Agric. Eng.* **2018**, *58*, 91–100.
33. Lara, L.; Rostagno, M. Impact of heat stress on poultry production. *Animals* **2013**, *3*, 356–369. [CrossRef] [PubMed]
34. Cai, Z.; Vasconcelos, N. Cascade R-CNN: Delving into high quality object detection. In Proceedings of the 2018 IEEE/CVF Conference on Computer Vision and Pattern Recognition, Salt Lake City, UT, USA, 18–23 June 2018; pp. 6154–6162.
35. Bai, Q.; Gao, C.; Zhao, C.; Li, Q.; Wang, R.; Li, S. Multi-scale behavior recognition method for dairy cows based on improved YOLOV5s network. *Trans. Chin. Soc. Agric. Eng.* **2022**, *38*, 163–172. [CrossRef]
36. Moez, K.; Alaeddine, M.; Mohammed, Y.; Wilfried, Y.; Tarik, N. Are formal methods applicable to machine learning and artificial intelligence? In Proceedings of the 2022 2nd International Conference of Smart Systems and Emerging Technologies (SMARTTECH), Riyadh, Saudi Arabia, 9–11 May 2022; pp. 48–53. [CrossRef]
37. Ramakrishnan, R.; Nikhil, G.; Yogananda, J. Framework for formal verification of machine learning based complex system-of-systems. *Insight* **2023**, *26*, 91–102. [CrossRef]
38. Tullo, E.; Fontana, I.; Fernandez, A.; Vranken, E.; Guarino, M. Association between environmental predisposing risk factors and leg disorders in broiler chickens. *J. Anim. Sci.* **2017**, *95*, 1512–1520. [CrossRef]

Disclaimer/Publisher's Note: The statements, opinions and data contained in all publications are solely those of the individual author(s) and contributor(s) and not of MDPI and/or the editor(s). MDPI and/or the editor(s) disclaim responsibility for any injury to people or property resulting from any ideas, methods, instructions or products referred to in the content.